THE INFLUENCE OF SOIL ORGANIC MATTER AGE SPECTRUM ON THE RECONSTRUCTION OF ATMOSPHERIC ^{14}C LEVELS VIA STALAGMITES

J Fohlmeister[1] • B Kromer • A Mangini

Heidelberg Academy of Sciences, c/o Institute for Environmental Physics, INF 229, 69120 Heidelberg, Germany.

ABSTRACT. The imprint of the radiocarbon bomb peak was detected in the top of stalagmite ER-77 from Grotta di Ernesto (NE Italy). This recently grown stalagmite reveals a reservoir age, also known as dead carbon fraction (dcf), of ~1050 ^{14}C yr, or 12%. By applying a ^{14}C soil-karst model, the age spectrum of soil organic matter (SOM) as well as the CO_2 contribution of the single SOM reservoirs to the total soil CO_2 can be derived. Under the assumption of constant vegetation, meaning both vegetation density and the age spectrum of SOM, it is possible to derive the soil-air ^{14}C activity of the past using the ^{14}C calibration curve (IntCal04). Hence, it is also possible to calculate an artificial stalagmite ^{14}C data set covering the last 25,000 yr with parameters determined for stalagmite ER-77. With this artificially constructed data set, we derived the hypothetical atmospheric ^{14}C activity by using the common method of applying a constant dcf on the modeled ^{14}C data set of the stalagmite. This theoretical approach allows to analyze the impact of a constant and variable SOM age spectrum on atmospheric ^{14}C reconstructions performed with real stalagmite ^{14}C measurements. We observe deviations between IntCal04 and the atmospheric ^{14}C activity as derived with our modeled ^{14}C data set, which are larger for older SOM than for younger SOM and vary in time up to 2 pMC, depending on the strength of the variations in the atmospheric ^{14}C level. This value is comparable with the 1-σ uncertainty given by IntCal04 for the last glacial. For a varying SOM age spectrum, the deviations between the calibration curve and ^{14}C level of the atmosphere reconstructed with a stalagmite exceed 3 pMC, which is larger than the 1-σ uncertainty of IntCal04. In general, the SOM has smoothing, shifting, and ^{14}C-depleting effects on the stalagmite ^{14}C record and, therefore, on the stalagmite-derived atmospheric ^{14}C activity. In this study, changes in soil-air pCO_2 and carbonate dissolution conditions, which have also an important impact on the ^{14}C record of a stalagmite, are not accounted for.

INTRODUCTION

Soon after the discovery of the carbon radionuclide by Libby et al. (1949) the measurements of radiocarbon in speleothems began. Franke (1951), Franke et al. (1959), Broecker at al. (1960), Hendy and Wilson (1968), and Geyh and Franke (1970) were among the first who used ^{14}C embedded in stalagmites calcite to date speleothems. Only a short time later, it was recognized (Hendy and Wilson 1968; Hendy 1970) that the most serious difficulty is the estimation of the initial ^{14}C activity of the carbon in the calcite, because the carbon embedded in stalagmites has 2 main sources and underwent a multiplicity of isotope-changing processes.

The 2 main sources of carbon atoms in stalagmite calcite originate either from CO_2 of the soil air, which is produced by microbial degradation of dead soil organic matter (SOM) and root respiration, or from the $CaCO_3$ of the host rock overlaying the cave system. After penetration through the upper soil zone, the meteoric water is in chemical and isotopic equilibrium with the partial pressure of CO_2 (pCO_2) in soil air, i.e. the carbon is present in the water as aqueous CO_2, bicarbonate (HCO_3^-), and carbonate (CO_3^{2-}). The ^{14}C composition of soil water depends on the ^{14}C activity of the soil-air pCO_2. The soil-air ^{14}C activity in turn depends on the ^{14}C incorporated in organic matter, which is near the atmospheric ^{14}C value of the time of photosynthesis of the plants and on the age composition of the different compartments of SOM (Dörr and Münnich 1986; Harrison et al. 1993; Trumbore 2000). Accounting for the relatively small ^{14}C fractionation from gaseous CO_2 to dissolved inorganic carbon (DIC), the ^{14}C in the DIC of soil water is near atmospheric ^{14}C activities. When the acidic soil water enters the karst aquifer, it dissolves the host-rock carbonates. In general, the host rock is very old and, hence, its ^{14}C is completely depleted ("dead carbon"). Usually, an *a priori* unknown fraction of dead carbon is injected into the water dripping onto the stalagmite during carbonate dissolution. Depending on the carbonate dissolution system and on soil-air pCO_2, it is possible to inject 0–50% dead carbon into a stalagmite (Garrels and Christ 1965; Hendy 1970, 1971;

[1]Corresponding author. Email: jens.fohlmeister@iup.uni-heidelberg.de.

99

Salomons and Mook 1986; Schwarcz 1986). Thus, a ^{14}C age uncertainty of up to one ^{14}C half-life can be introduced.

The large range of dead carbon injection and the corresponding age uncertainty can be explained, if the condition of the host-rock carbonate dissolution is investigated in more detail. Dissolution can occur under 2 extreme cases (open or closed carbonate dissolution) or under intermediate conditions (e.g. Wendt et al. 1967; Hendy 1970; Wigley 1975; McDermott 2004). In a closed system, the aqueous solution has no contact with the infinite soil CO_2 reservoir during the dissolution process. Therefore, for each mole of carbonate dissolved from the acid hydrolysis of the host rock, 1 mole of CO_2 is converted to bicarbonate, according to $CaCO_3 + CO_2 + H_2O \rightarrow Ca^{2+} + 2HCO_3^-$. When the solution becomes saturated with respect to calcite, approximately half of the carbon atoms originate from the carbonate rock, which is devoid of ^{14}C, and the other half is derived from soil-air CO_2 with a ^{14}C activity similar to the atmospheric composition (Hendy 1971). When the carbonate dissolution occurs in an open system, the aqueous solution is in isotopic equilibrium with the unlimited reservoir of soil gaseous carbon dioxide. In the dissolution process, carbon isotope exchange between DIC and soil-air CO_2 controls the ^{14}C activity of karst water, which is, hence, similar to that of the soil-air CO_2. In real soil-rock-cave systems, the carbonate dissolution occurs in conditions that are intermediate between a completely open and completely closed system. The behavior of the carbonate dissolution system is *a priori* unknown and complicates the ^{14}C dating of stalagmites.

The rise of U/Th dating techniques (Edwards et al. 1987; Li et al. 1989; Scholz and Hoffmann 2008) allowed an absolute age determination of stalagmites and ^{14}C analysis of stalagmites became interesting again, because from now on it was possible to use ^{14}C as a geochemical tracer. An important application was the detection of the atmospheric ^{14}C bomb peak imprinted in stalagmites (Genty and Massault 1997, 1999; Genty et al. 1998; Mattey et al. 2008; Smith et al. 2009), which allowed the possibility to investigate the carbon transfer dynamics of the soil and karst above caves. Furthermore, the condition of carbonate dissolution could be derived by the proportion of the dead carbon (e.g. Genty et al. 1999, 2001; Beck et al. 2001). A more sophisticated extension of this approach was to use the carbon radionuclide in stalagmites in order to extend the ^{14}C calibration curve (e.g. Beck et al. 2001; Hoffmann et al. 2010). The most widespread approach to reconstruct the atmospheric ^{14}C activity by stalagmites is to measure the reservoir age of the stalagmite, also known as dead carbon fraction (dcf), in times of known atmospheric ^{14}C activity. The atmospheric ^{14}C activity in times of interest is then determined by measuring ^{14}C in stalagmites at an appropriate time interval and using the known dcf, which is assumed constant in time (Vogel and Kronfeld 1997; Geyh and Schlüchter 1998; Genty et al. 1999; Goslar et al. 2000; Beck et al. 2001).

In this paper, we investigate the errors introduced by applying such a method even under constant conditions in the various carbon reservoirs and processes occurring before the calcite of a stalagmite precipitates. Lacking a stalagmite covering long time intervals, we focus on a more theoretical point of view. In order to be able to evaluate the errors arising with such an approach, we present the measurements of the imprint of the ^{14}C bomb peak detected in stalagmite ER-77 of Grotta di Ernesto (NE Italy). Then, the complex approach of Genty and Massault (1999) is used to infer the age spectrum of SOM in the soil above the cave. However, this step should only motivate the choice of the SOM parameters. The more important step is that afterwards an artificial data set of ^{14}C is calculated that mirrors the ^{14}C activity in a stalagmite. The artificial ^{14}C data set was modeled with the Genty and Massault (1999) method using the estimated SOM characteristics for the Grotta di Ernesto stalagmite and the atmospheric ^{14}C record (IntCal04; Reimer et al. 2004). In fact, in the model we fixed temperature (and therefore the fractionation constants), the carbonate dissolution system, the soil-air pCO_2, and the age spectrum of SOM. In the next step, we infer the atmospheric ^{14}C activities from

the artificially constructed ^{14}C data set using a previously determined dcf from the recent literature. In other words, we compare the more comprehensive and reality reflecting Genty and Massault (1999) model of ^{14}C incorporation in stalagmites with the simple approach of a constant dcf. With this method, we are able to focus on the systematic deviations between the atmospheric ^{14}C activity derived by a stalagmite and the atmospheric ^{14}C activity as published in IntCal04. This study should not be understood to improve the ^{14}C calibration curve. This model approach aims to estimate the uncertainties introduced by the reconstruction of atmospheric ^{14}C activities with stalagmites.

MODELING RADIOCARBON IN STALAGMITES

In order to evaluate the ^{14}C measurements of stalagmite ER-77, we used the model of Genty and Massault (1999). The model includes all processes for ^{14}C involved in stalagmite growth. This allows translating the ^{14}C activity of the atmosphere ($^{14}C_{atm}$) into a ^{14}C signal recorded in the stalagmite. We then check under which parameters the model fits the data (see below). The model takes into account that the SOM contains several reservoirs (Dörr and Münnich 1986; Harrison et al. 1993; Tegen and Dörr 1996). Following the approach of Genty and Massault (1999), we divide the SOM into 3 reservoirs of different ages. This includes 1 fast reservoir with an age of y_1 years that inject $^{14}CO_2$ to the total soil-air CO_2, which has a mean atmospheric ^{14}C activity of the last y_1 years. Within the model, we define also 1 medium (slow) reservoir, y_2 (y_3), which produces $^{14}CO_2$ with a mean ^{14}C activity similar to the mean atmospheric ^{14}C activity between the years y_1 and y_2 (y_2 and y_3). All ^{14}C activities used for the calculations are decay-corrected with respect to the year of soil-air CO_2 production, although on timescales of ~100 yr this step could be neglected. Each reservoir contributes c_i ($i = 1, 2, 3$) fractions to the total soil CO_2 with

$$c_1 + c_2 + c_3 = 1 \qquad (1)$$

and gives the mean decay-corrected soil-air ^{14}C activity ($a^{14}C_g$, in units of percent modern carbon: pMC), which is in isotopic equilibrium with soil water:

$$a^{14}C_g = c_1 \times (a^{14}C_{y1}) + c_2 \times (a^{14}C_{y2}) + c_3 \times (a^{14}C_{y3}) \qquad (2)$$

where $a^{14}C_{yi}$ ($i = 1, 2, 3$) are the mean decay-corrected atmospheric ^{14}C activities. We use the fact that at pH values around 7 to 8, typical for groundwaters in karst aquifers (Dreybrodt 1988), nearly all carbon is bounded in molecules as bicarbonate (HCO_3^-). This allows calculating the ^{14}C activity of dissolved inorganic carbon ($a^{14}C_{DIC}$) in equilibrium with soil-air CO_2 as

$$a^{14}C_{DIC} = a^{14}C_g + 0.23 \times {}^{13}\varepsilon_{b-g} \text{ [pMC]} \qquad (3)$$

using the carbon isotope enrichment factor of ^{13}C between gaseous CO_2 and HCO^-_3 (${}^{13}\varepsilon_{b-g}$) given by Mook and de Vries (2000) and the relationship between ^{13}C and ^{14}C activity ($0.23 \times {}^{13}\varepsilon_{b-g}$) as suggested by Saliège and Fontes (1984).

In the next step, we calculate the ^{14}C activity of the water after the solution is saturated with respect to calcite ($a^{14}C_{sat}$) by using the $dc_{calcite}$ parameter. This value parameterizes the dead carbon, which is introduced in the solution by calcite dissolution and is given in percent:

$$a^{14}C_{sat} = (1 - dc_{calcite} / 100) \times a^{14}C_{DIC} \text{ [pMC]} \qquad (4)$$

$dc_{calcite}$ is a measure of the degree of the open and closed carbonate dissolution condition. If $dc_{calcite}$ is 0%, the dissolution occurs under open conditions, whereas a $dc_{calcite}$ ~50% represents closed con-

ditions. The ^{14}C activity of the stalagmite ($a^{14}C_{stal}$) is then determined by fractionation between the bicarbonate and the precipitating calcite ($0.23 \times {}^{13}\varepsilon_{c-b}$):

$$a^{14}C_{stal} = a^{14}C_{sat} + 0.23 \times {}^{13}\varepsilon_{c-b} \ [pMC] \tag{5}$$

The total dcf is then defined as

$$dcf = (1 - a^{14}C_{stal} / a^{14}C_{atm}) \times 100 \ [\%] \tag{6}$$

The total dcf is a mixture of the dead carbon originating from host-rock carbonate and from the soil organic matter and is slightly modified by carbon isotope fractionation effects between gaseous CO_2, HCO^-_3, and $CaCO_3$.

CHOICE OF MODEL PARAMETERS

Cave Site

Grotta di Ernesto is a shallow cave located 1167 m asl in northeast Italy, south of the Dolomites. The cave is overlain by 5–30 m of dolomitic limestone. It is ideally suited because it is small, largely undisturbed, and one of the most extensively monitored cave sites worldwide (e.g. Borsato 1997; McDermott et al. 1999; Huang et al. 2001; Frisia et al. 2003; Borsato et al. 2007). The hillslope vegetation above the cave consists of C_3 plants, mostly conifers, seasonal shrubs, and grass.

Over the whole year, the cave temperature is 6.6 °C. The 30-yr average of 1300 mm annual precipitation measured at the nearby meteorological station Vezzena shows a bimodal distribution with maxima during spring and autumn. Taking into account evapotranspiration (calculated after Thornthwaite 1948), the highest soil infiltration occurs in autumn. Snow is usually present in the winter months and melts during March and April, resulting in an important infiltration event. The karst aquifer reservoir, which feeds the drips in the cave beneath, is in equilibrium with mean annual soil-air pCO_2 (Fairchild et al. 2000; Frisia et al. 2005).

Sample Preparation

We investigated the ^{14}C content in the top section of stalagmite ER-77. This stalagmite is continuously annually laminated (Frisia et al. 2003) from the year of removal (1992) back to AD 1713. The chronology was reconstructed by counting back in time each visible lamina. The upper 150 laminae, which correspond to the 150 yr before AD 1992, are typically ~100 μm thick and are stacked regularly to form a columnar fabric.

We took 17 subsamples from the top 13 mm of the stalagmite using a micromill. The subsamples were milled by using a 0.3-mm dental burr. Unfortunately, it was not possible to drill the samples in a CO_2-free atmosphere due to technical limitations. However, the background used (Iceland spar) does not show a significant enrichment in ^{14}C than other background samples, which usually were drilled under a CO_2-free atmosphere. Therefore, we believe the samples are not affected by the recent atmospheric $^{14}CO_2$. With a spatial resolution of 0.6 mm, we achieved a sample mass of roughly 8 mg calcite each, resulting in a temporal resolution of 4 yr (in the 1970s) up to 10 yr (in the 1890s) depending on the growth rate. The calcite powder was acidified under vacuum and the emerging CO_2 gas was captured. The CO_2 was then combusted to carbon, which was pressed into cathodes for accelerator mass spectrometry (AMS) analysis. The ^{14}C measurements were performed at the University of Lund AMS facility (Skog 2007). A more detailed subsample treatment can be found in Fohlmeister et al. (2010). Results of the ^{14}C measurements are listed in Table 1.

Table 1 Radiocarbon data of stalagmite ER-77.

Label	Distance from top (mm)	Year (AD)	Age error (yr)	a^{14}C (pMC)	1-σ error
A	12.62	1888.87	5	87.9	0.35
B	12.02	1898.67	4.38	86.96	0.38
C	11.43	1905.99	3.27	87.01	0.35
D	10.83	1911.92	2.86	88.02	0.36
E	10.23	1917.69	2.48	87.47	0.35
F	9.63	1922.27	2.37	87.26	0.35
G	9.04	1926.29	1.94	—	—
H	8.44	1930.89	2.52	87.3	0.34
I	7.84	1935.65	2.21	87.04	0.34
J	7.24	1939.6	2.04	87.52	0.36
K	6.65	1944.53	2.79	86.76	0.36
L	6.05	1950.08	2.55	86.7	0.36
M	5.45	1955.03	2.37	—	—
N	4.86	1960	2.48	87.61	0.34
O	4.26	1964.34	1.8	91.26	0.34
P	3.66	1967.62	1.85	106.88	0.4
Q	3.06	1971.42	2	118.19	0.42
R	2.47	1975.43	1.8	119.07	0.44
S	1.87	1979.63	2.42	112.79	0.44

Modeling the Age Spectrum of SOM above Grotta di Ernesto

With the soil-karst model for ^{14}C (Equations 1–5) and with the knowledge of atmospheric ^{14}C concentration of the last ~150 yr (Levin and Kromer 2004; Reimer et al. 2004), we are able to calculate the stalagmites ^{14}C activity in dependence of the parameters dc$_{calcite}$, y_i, and c_i (i = 1, 2, 3). The parameter determination of the SOM age spectrum is performed in an iterative way consisting of 2 steps. First, the fraction of dead carbon originating from the host rock is calculated (dc$_{calcite}$). The dc$_{calcite}$ is determined by the mean difference between the atmospheric ^{14}C activity and the stalagmite ^{14}C measurements performed at the depths corresponding to the years AD 1890 to 1950 with an *a priori* arbitrary but reasonable set of y_i and c_i (e.g. taken from studies estimating soil parameters with a similar vegetation cover). In this period of nearly constant atmospheric ^{14}C activities, the choice of the age spectrum parameters leads only to a constant offset. Knowing the "preliminary" host-rock dead carbon, the age spectrum of SOM is determined by using the ^{14}C measurements of the stalagmite, which correspond to the period of the bomb peak between AD 1950 to 1980. The parameters y_i and c_i are found by minimization of the deviation between the model data set and the ^{14}C measurements of the stalagmite in the bomb peak period. Then it is necessary to reevaluate the host-rock dead carbon, due to changes of the vegetation induced dead carbon. After that, the vegetation parameters are adjusted again. This iteration was done until the deviations of the model output were minimized compared to the ^{14}C values measured in the stalagmite. The modeled ^{14}C activity of the stalagmite with the best-fitting parameters is shown in Figure 1.

We found that the dead carbon originating from the host-rock carbonate is 13.7%. The fractionation is responsible for an enrichment of ~2.3 pMC (dead carbon fraction of about –2.02%). The dead carbon contribution of the vegetation is 0.09% between 1800 and 1950. This results in a mean total dcf of 11.77% in this period. This value is in agreement with the one found for the younger part (1800–1900) of the nearby stalagmite ER-76 (unpublished data). In addition, this value is consistent with
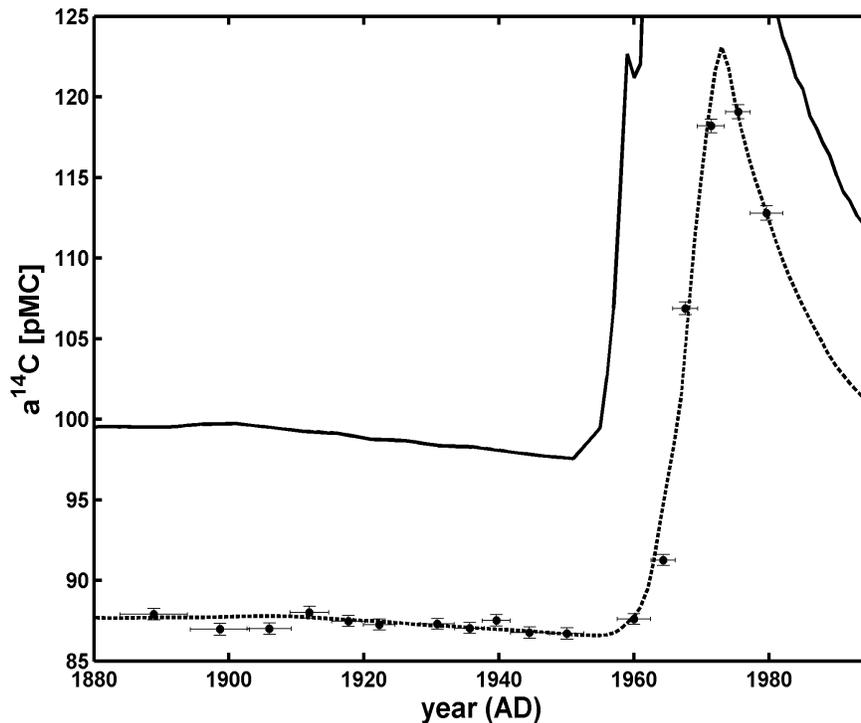
Figure 1 The atmospheric ^{14}C activity (straight line) shows a plateau before AD 1950, followed by the bomb pulse anomaly. The stalagmite data (black circles) are shown with 1-σ uncertainty in the ^{14}C measurements and with a width of the micromilled area of the stalagmite converted to an age. The best-modeled fit of the measured data is depicted by the dashed line.

the values given in other studies (e.g. Genty et al. 1997; Beck et al. 2001). The best-parameterized age spectrum of the SOM to fit the stalagmite ^{14}C measurements is then found to be:

- $y_1 = 5$ yr; $c_1 = 0.07$.
- $y_2 = 11$ yr; $c_2 = 0.53$.
- $y_3 = 100$ yr; $c_3 = 0.4$.

These values allow computing the soil-air ^{14}C activity for each year. For 2006, for example, the soil-air ^{14}C activity is calculated as 110.6 pMC, which is higher than the ^{14}C activity of the free atmosphere at this time (~106 pMC, Levin et al. 2010). In contrast, in 1963 the soil-air ^{14}C activity was 106.5 pMC, which was much lower than the ^{14}C activity of the atmosphere at this time. In 1952, after a long time of a rather stable atmospheric ^{14}C activity, the ^{14}C activity of the soil-air (98.1 pMC) is similar to atmospheric values. This shows that after a time of increasing atmospheric ^{14}C activity, the soil air has generally lower values than the atmosphere, while the relationship is inversed at times with decreasing atmospheric ^{14}C activities. However, this example deals with the unique strong and fast atmospheric ^{14}C variation, which originates due to the atomic weapon tests of the mid-20th century. The differences in ^{14}C activity between the atmosphere and soil air are much smaller for natural variations in the atmospheric ^{14}C activity.

The derived soil parameters are consistent with previously published values of areas with a similar vegetation cover as present above Grotta di Ernesto. Dörr and Münnich (1986) proposed for the

short-living fraction 5 yr and for the long-living fraction ~100 yr for soils in the Rhine Valley. Tegen and Dörr (1996) proposed approximately the same values for several soils covered by forest in southwest Germany. Both studies analyzed also the proportion to the overall soil-air CO_2 and found that for the winter season the impact of the old organic matter is more important than the young material. This confirms our findings of c_1, c_2, and c_3 if one considers that mainly the autumn and winter precipitation charge the water aquifer, due to high evapotranspiration in spring and summer (Frisia et al. 2003; Wackerbarth et al. 2010). Furthermore, for Grotta di Ernesto it is assumed that the stalagmites grow mainly in the winter months due to the high oversaturation between drip water and cave air pCO_2 (Frisia et al. 2003, 2011). In climatic areas different from those in central Europe, Trumbore (2000) investigated forested soils in boreal forests and found turnover times of 60 yr representing the surface moss and detritus SOM and ~1000 yr for other organic matter in the humic layer. In tropical forests, Trumbore (2000) gives turnover times for 3 reservoirs: 3, 30, and >6000 yr.

Most likely, other values for soil parameters at Grotta di Ernesto can be excluded to describe the behavior of all measured stalagmite ^{14}C samples. On the one hand, the system has 7 variables and only 1 equation (Equation 1), but on the other hand, the long, middle, and short reservoir ages are well decoupled. The young reservoir is responsible for the time delay between the increase of atmospheric and stalagmite ^{14}C activities. The reservoir with the intermediate age is responsible for the gradient of the ^{14}C increase in the stalagmite. The declining ^{14}C level in the post-bomb period in the sinter is determined by the age and proportion of the oldest reservoir. The mix of all soil reservoirs can explain the timing and the shape of the ^{14}C maximum in the stalagmite.

RADIOCARBON CALIBRATION CURVE DERIVED FROM A STALAGMITE

The aim of many studies has been to refine and to extend the ^{14}C calibration curve using stalagmites (Vogel and Kronfeld 1997; Geyh and Schlüchter 1998; Genty et al. 1999; Goslar et al. 2000; Beck et al. 2001; Hoffmann et al. 2010). For that purpose, a ^{14}C profile along the stalagmites growth axes is measured. The reservoir age (or dcf) is then determined by comparing ^{14}C measurements of the stalagmite with the known atmospheric ^{14}C levels. The mean dcf with the corresponding standard deviation was calculated and applied on ^{14}C measurements of the stalagmite in time intervals where the calibration curve needs to be improved. In this section, we will show the uncertainties and differences in the atmospheric ^{14}C curve derived by a stalagmite compared to IntCal04, even if all climate and process parameters are constant over time, which is a necessary assumption in those studies. We will attribute the differences to the composition of the vegetation and SOM above the cave.

In the following theoretical study, we do not use a measured stalagmite ^{14}C record. We only use IntCal04, which covers a time interval from 26,000 yr before present (kyr BP) to AD 1950, and the model proposed above (Equations 1–5), which proved to fit the ^{14}C measurements of the 20th century bomb pulse very convincingly, to construct an artificial ^{14}C data set representing ^{14}C measurements on a stalagmite. We focus on the last 25,000 yr to be able to use the prior 1000 yr for allocating a ^{14}C signature to SOM, which may has an age of 1000 yr. Changes in the open versus closed carbonate dissolution condition are neglected. Furthermore, we do not account for variations in soil-air pCO_2. Both aspects have a large potential to change the amount of dead carbon, which is incorporated to the stalagmites (Garrels and Christ 1965; Wendt et al. 1967; Hendy 1971; Wigley 1975; Salomons and Mook 1986; Dulinski and Rosanzki 1990). This is therefore a simplistic approach on variations in soil-air pCO_2 and dissolution conditions; however, this strategy allows attributing changes in the stalagmite ^{14}C activity to the influence of the SOM ^{14}C activity. This artificial ^{14}C data set replaces real measurements, and we can be sure that neither the age spectrum of SOM nor the soil pCO_2 or the way of carbonate dissolution has changed.

The procedure to derive the atmospheric ^{14}C activity from the artificially constructed stalagmite data set is performed as described above. We calculate the dcf of the stalagmite following Equation 6 in the time interval from 12 to 0 kyr BP and average the dcf over time. Then, we apply the mean dcf in the period between 25 to 12 kyr BP to derive the atmospheric ^{14}C activity. We then compare the IntCal04 atmospheric ^{14}C activity with the ^{14}C activity derived from the modeled ^{14}C data set.

Constant Composition of SOM

In a first step, we keep the vegetation composition and SOM age spectrum constant over time to compute the artificial stalagmite ^{14}C data set. We calculate the ^{14}C activity derived by the stalagmite as explained above. Then, we focus on the changes of the modeled stalagmite ^{14}C data set compared to the atmospheric ^{14}C curve and show which differences between the atmospheric ^{14}C activity derived by the modeled ^{14}C data set and the atmospheric ^{14}C level, given by IntCal04, are introduced by using a constant dcf. Our first example is the relatively young SOM age spectrum we derived for Grotta di Ernesto. We calculate, with Equations 1–5 and the parameters derived for the top section of the stalagmite ER-77, the artificial ^{14}C data set of a stalagmite (Figure 2a). The last 12 kyr were used to determine the total dcf (Figure 2b) by applying Equation 6. In this time interval, the mean dcf is $12.06 \pm 0.23\%$. We detect a small linear trend in the dcf even under complete constant conditions. The slope of this trend is $0.21\%/10$ kyr.
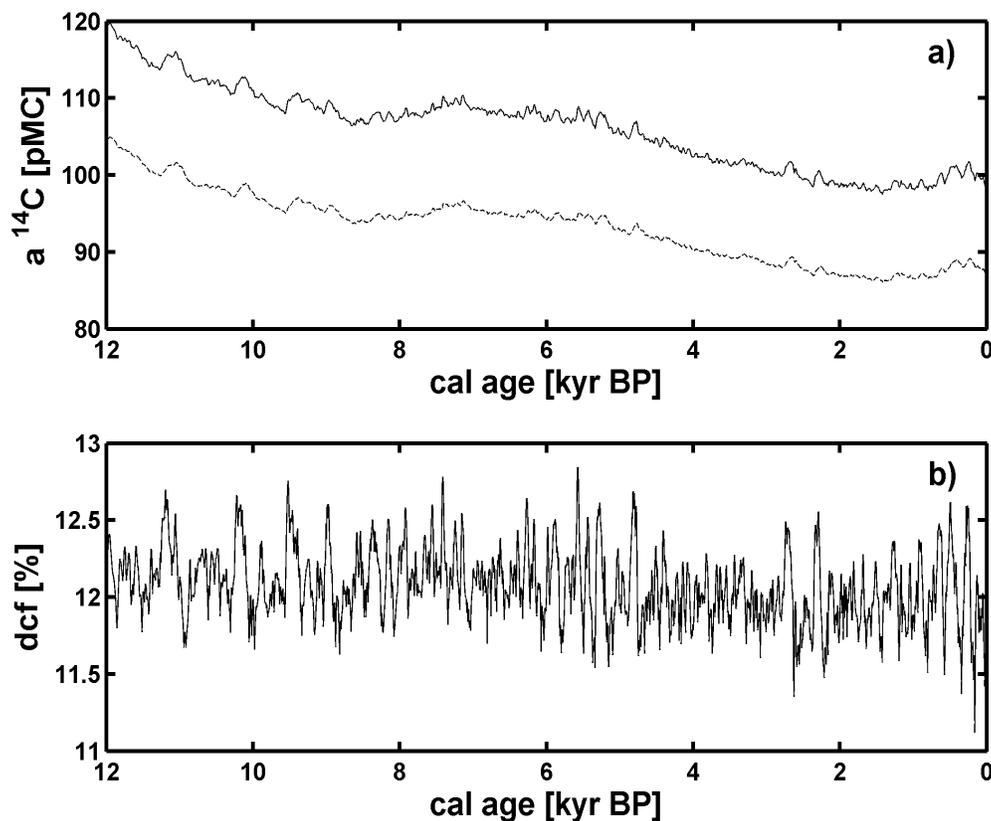

Figure 2 a) IntCal04 (solid line) and the modeled ^{14}C data set (dashed line). The modeled ^{14}C data set is smoothed compared to IntCal04 due to the influence of the SOM age spectrum. b) The calculated dcf of the time series presented in (a). The mean dcf of this period is $12.06 \pm 0.23\%$.

The dcf varies between about 11.1% and 12.8% (Figure 2b). The maximum and minimum values of the dcf arise due to the autocorrelation characteristics of ^{14}C in the soil-air CO_2, which is induced by the age spectrum of the SOM. The model (Equations 1–5) we used to construct the artificial ^{14}C data set of a stalagmite, accounts for the ^{14}C autocorrelation of the SOM, while the dcf is computed from the atmospheric ^{14}C values and lacks such memory. This implies that where the atmospheric ^{14}C activity increases (decreases), the SOM introduces less (more) ^{14}C to the soil-air CO_2 compared to the atmospheric ^{14}C content at that time, because when the plants grew, the atmosphere had a smaller (higher) ^{14}C content. Therefore, the maxima (minima) in the ^{14}C activity recorded in the stalagmite appear delayed compared to the maxima (minima) of the atmospheric ^{14}C activity. These delays cause the apparent variations of the dcf. However, the delay is also responsible for the timing of the extreme values in dcf, which occur simultaneous with the extreme values of the atmospheric ^{14}C activity. Furthermore, plateaus after an atmospheric ^{14}C increase (decrease) result in a decreasing (increasing) dcf, which is also caused by the SOM induced time delay. In addition, we observe that the faster and the more distinct the atmospheric ^{14}C varies, the larger the changes in dcf are.

We use the mean dcf of the last 12 kyr to derive the atmospheric ^{14}C curve with the artificially constructed ^{14}C data set (Figure 3a, dashed line) for the period between 25 to 12 kyr BP. The difference between IntCal04 (Figure 3a, solid line) and the atmospheric ^{14}C curve derived by the modeled ^{14}C data set of the stalagmite (Figure 3a, dotted line) shows a mean offset in this period of 0.63 pMC (Figure 3b) and peaks at a maximum with 1.3 pMC at 19.45 kyr BP and with 2 main minimum values at 12.43 and 19.65 kyr BP (–0.4 and –0.2 pMC). The small slope in the deviation between the level of the atmospheric ^{14}C activity derived from the stalagmite and IntCal04 is due to the neglected linear trend in the dcf during the last 12 kyr.

Figure 3 shows that this approach leads to an underestimation of the real atmospheric ^{14}C activity and would yield on average ~60 ^{14}C yr older values during the whole period. The apparent aging is attributed to the neglected linear trend in dcf and to the mean turnover time of vegetation, allowing for decay of ^{14}C before the SOM decomposes. Furthermore, the atmospheric ^{14}C curve derived from the synthetic data set is smoothed compared to IntCal04. This smoothing is due to the age spectrum of SOM above the cave, which is not accounted for in the usual way of atmospheric ^{14}C level reconstructions from stalagmites (Equation 6). The smoothing is more pronounced in periods of fast and large atmospheric ^{14}C level variations. This means that faster and larger variations in the atmospheric ^{14}C levels are accompanied by larger deviations between the real atmospheric ^{14}C level and the reconstructed atmospheric ^{14}C activity derived from the stalagmite. In fact, during periods of increasing ^{14}C activities in the stalagmite the deviations peak in a maximum, while during periods of decreasing ^{14}C activities in the stalagmite the deviations peak in a minimum.

The 1-σ error of IntCal04 at 25 to 15 kyr BP is between ±1.5 and ±2.5 pMC. This uncertainty range would cover completely the observed deviations between the stalagmite-derived atmospheric ^{14}C activity and IntCal04. Nevertheless, calibration of ^{14}C ages with the ^{14}C curve derived from the artificial data set would yield differences of about –24 to +100 yr compared to calibration of the same ^{14}C ages with IntCal04.

The age spectrum of vegetation and SOM above Grotta di Ernesto represents a cold climate typical to its elevation of ~1100m asl in central Europe and the mean annual temperature of ~6.6 °C. Obviously, the atmospheric ^{14}C curve derived by a stalagmite would look different if we assume to have a soil above the cave covered by vegetation and SOM with an older age spectrum, representing a warmer climate. For this scenario, we chose an age spectrum of SOM valid for a warmer climate. We followed the values published in Trumbore et al. (1995) and Trumbore (2000) for the East Ama-
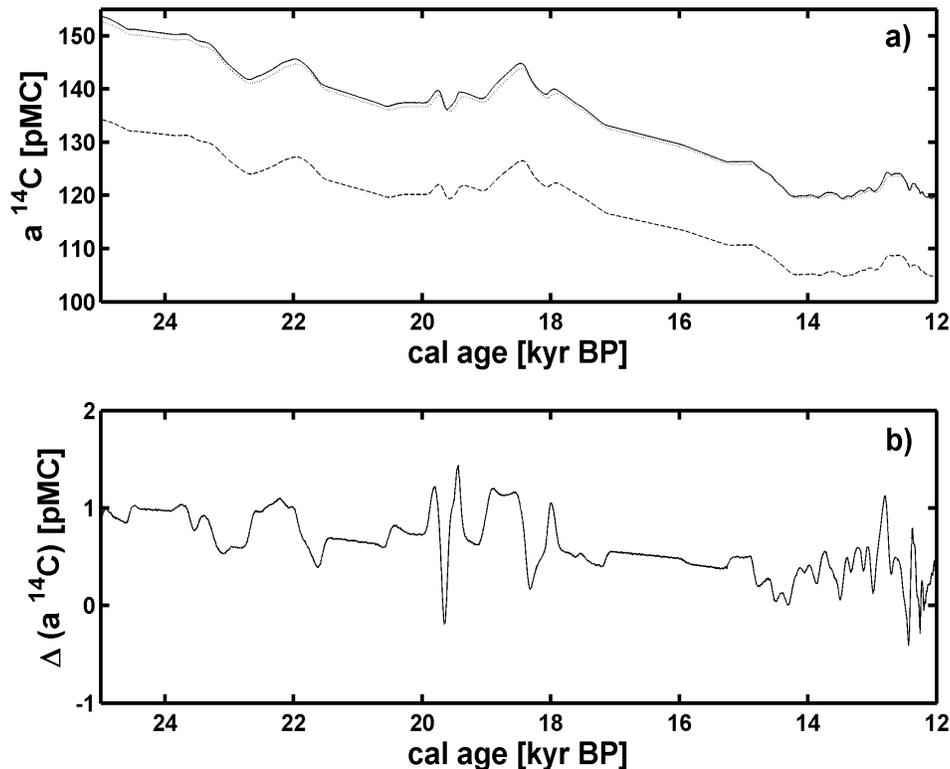
Figure 3 a) As in Figure 2a, IntCal04 (solid line) and the modeled ^{14}C data set (dashed line) are shown. Applying the mean dcf determined in the last 12 kyr results in the reconstructed atmospheric ^{14}C curve (dotted line). b) The deviations of the reconstructed atmospheric ^{14}C curve from IntCal04 in the period between 26 and 12 kyr BP. A decreasing trend in the offset is observed. The maximum offset is 1.3 pMC (at ~19.45 kyr BP).

zonian forest, with ages of SOM: $y_1 = 3$, $y_2 = 30$, and $y_3 = 1000$ yr and contributions to the total soil-air CO_2: $c_1 = 0.21$, $c_2 = 0.57$, and $c_3 = 0.22$. We set y_3 to 1000 yr in order to be able to deal with the last 25 kyr, although the slow reservoir is expected to be older. We applied for these computations the same $dc_{calcite}$ of 13.7% and the same temperature of 6.6 °C as valid for Grotta di Ernesto in order to attribute all variations to the changed age spectrum of SOM. Figure 4a shows IntCal04 (solid line) and the modeled ^{14}C activity of the stalagmite (dashed line).

In Figure 4, similar but even more pronounced characteristics as for the younger SOM reservoir are observed. Hence, by applying an other age spectrum of the SOM, we show that the older the SOM reservoir, the more smoothed and delayed the ^{14}C activity, recorded in a stalagmite, will be when it is compared to the atmospheric ^{14}C activity (compare Figure 2a and Figure 4a). Changing to an old SOM reservoir results in a larger dcf and in variations in the dcf (between 12.3 and 13.9%) comparable to the observed dcf of the younger age spectrum of SOM. The mean dcf calculated in the last 12 kyr is 12.92 ± 0.26% (Figure 4b) for the older age spectrum of SOM. This corresponds to an increase in the dcf of ~0.9% compared to the simulation with stalagmite ER-77 parameters. This is mainly caused by additional ^{14}C decay due to the longer residence time for C in the slow reservoir. The variations in the dcf appear more structured than for the Ernesto type of SOM. This is the result of the longer memory of soil-air ^{14}C mainly induced by the age of the old proportion of SOM. In the next step, we use the mean dcf of the last 12 kyr for our calculations of the atmospheric ^{14}C activity
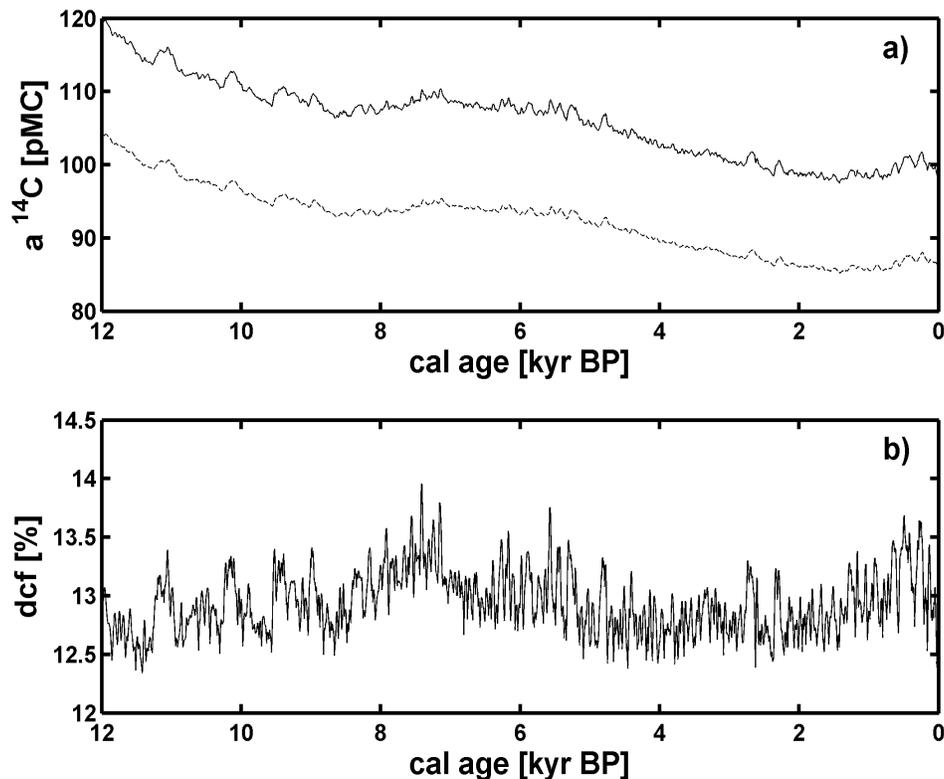
Figure 4 We calculated the dead carbon fraction (dcf; Equation 6) from the artificially constructed ^{14}C data set (dashed line) with the parameters $dc_{calcite}$ = 13.7% and y_1 = 3, y_2 = 30, and y_3 = 1000 yr; c_1 = 0.21, c_2 = 0.57, and c_3 = 0.22 and IntCal04 (solid line). b) Shows the temporal variation of the dcf, which ranges from 12.3 to 13.9%, resulting in a mean dcf of 12.92%.

derived with the artificially constructed ^{14}C data set (Figure 5a, dotted line) and finally to determine the deviations between IntCal04 and atmospheric ^{14}C activity derived with this data set (Figure 5b).

Compared to IntCal04 the ^{14}C activity of the atmosphere as derived from the stalagmite is in average 0.59 pMC lower. However, there are periods in which the atmospheric ^{14}C curve derived from the artificial data set is up to about 2.2 pMC lower than IntCal04 (at ~18.5 kyr BP). In other periods the atmospheric ^{14}C curve as constructed from the modeled stalagmite ^{14}C data set is about 0.5 pMC (14.3 kyr BP) higher than IntCal04. These deviations are larger than those derived for the younger soil parameters, as determined for Grotta di Ernesto, and exceed at certain time intervals the 1-error of IntCal04. The largest deviations between both curves appear simultaneous to the largest ^{14}C variations in IntCal04. As described above, the SOM disturbs the atmospheric ^{14}C signal. It leads to delay and to smoothing effects of the atmospheric extreme values. The delay and the smoothing are then recorded in the stalagmite (Figure 5a). When the artificial stalagmite ^{14}C data set is used to compute the atmospheric ^{14}C activity with the constant dcf approach, both, the delay and the smoothing characteristic of the SOM age spectrum, affects the timing and the amplitude of the peaks in the reconstructed atmospheric ^{14}C activity. Furthermore, we found, by comparing Figures 3b and 5b, that the larger the age spectrum of the soil above a cave, the larger the deviations from the real atmospheric ^{14}C activity.
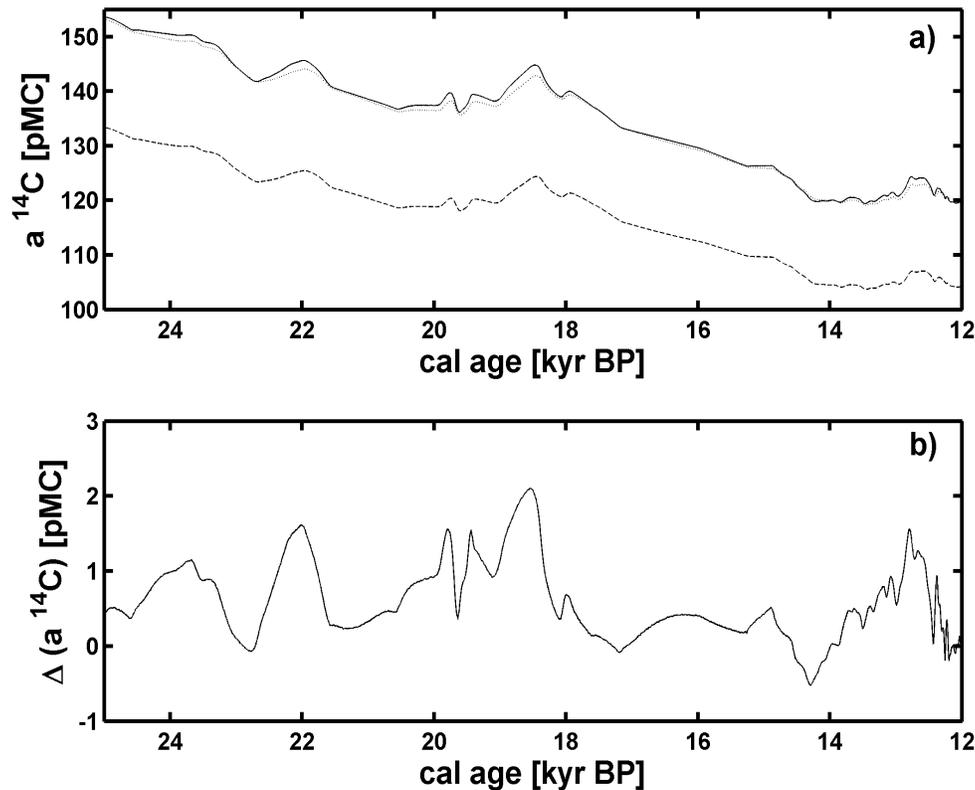
Figure 5 a) Applying the dcf value of 12.92% to the period between 25 and 12 kyr BP on the modeled ^{14}C data set (dashed line), we can calculate a reconstructed atmospheric ^{14}C curve (dotted line) and compare this with IntCal04 (solid line). In b) we show the deviations between IntCal04 and the reconstructed atmospheric ^{14}C activity. The mean deviation is 0.59 pMC with a minimum of about –0.5 pMC (at ~14.3 kyr BP) and with a maximum of ~2.2 pMC (at ~18.5 kyr BP).

Variations in the Composition of SOM

In most regions of the Earth, the climate changed during the last 25 kyr, resulting in a change of the vegetation composition in those areas. In particular, the vegetation modified during the termination of the last glacial maximum (LGM) from a cold-climate-adapted vegetation composition to a warmer-climate-adapted vegetation composition. Hence, we can improve the approach performed above by allowing the vegetation composition to change with time. The simplest approach is to assume a step function for the SOM age spectrum. We prescribed a constant vegetation composition in the Holocene and a constant vegetation composition during the LGM and the termination of the LGM. Hence, we apply the warmer-climate vegetation composition with the older SOM age spectrum (Trumbore 2000) to the period between 12 kyr BP to AD 1950 and a colder-climate vegetation composition coinciding with a younger SOM age spectrum (as derived from ER-77) from 25 to 12 kyr BP. We then perform the calculations as described above. First, we determine the mean dcf in the last 12 kyr with the warmer-climate vegetation composition, which is 12.92% (see Figure 4b). Afterwards, we apply this value for the colder period in order to reconstruct the level of the atmospheric ^{14}C curve with the artificial ^{14}C data set. That curve has ~0.78 pMC higher ^{14}C values compared to the IntCal04 calibration curve (Figure 6a and b).
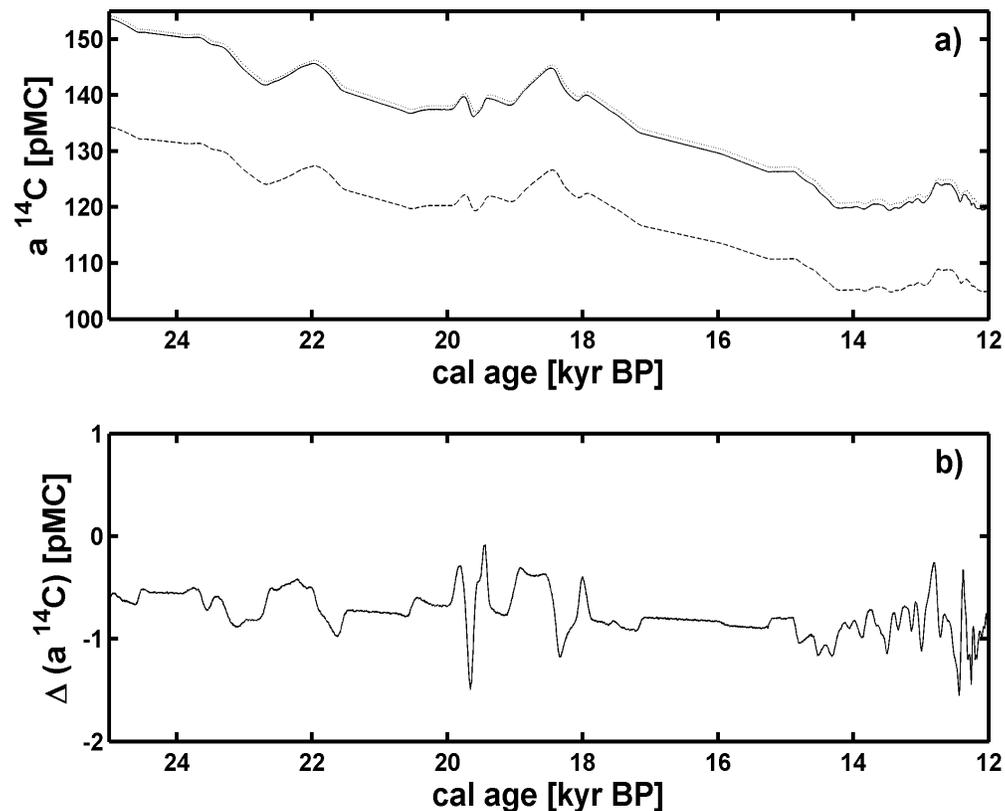
Figure 6 Assuming soil conditions, which is adapted for warmer climate for the last 12 kyr, results in a mean total dcf of 12.92%. a) IntCal04 (solid line) and the artificially constructed ^{14}C data set (dashed line) are compared to the reconstructed atmospheric ^{14}C activity (dotted line), which was computed with the mean dcf of the last 12 kyr. (b) The use of this dcf results in an overestimation of the atmospheric ^{14}C level in colder climate conditions.

This absolute value of the offset is larger compared to that of constant vegetation adapted to colder climate conditions during the complete last 25 kyr (Figure 3). Furthermore, the offset points to the opposite direction and shows nearly the same temporal variations (compared with Figure 3b). The effect of more ^{14}C in the stalagmite-derived atmospheric curve is due to the assumption of a constant dcf. The dcf was derived with an older age spectrum, introducing more dead carbon into the stalagmite due to more time of radioactive decay. However, when this dcf value is applied for the colder period, the dcf is overestimated due to the change of the SOM age spectrum to younger values, which introduces less dead carbon to the stalagmite.

This comparison can be done the other way around. For example, we can assume an older age spectrum for the period between 25 and 12 kyr BP and a younger one for the last 12 kyr. This scenario is more appropriate for regions with present-day subtropical savannah vegetation. Those regions have had, at least partly, denser vegetation during the LGM, which were nearly comparable with those of modern tropical rainforests. For that case, we calculated the mean dcf of the last 12 kyr to be 12.06% (Figure 2b). The calculations for the period between 25 and 12 kyr BP reveal that the atmospheric ^{14}C activity derived with the stalagmite is on average ~2 pMC lower than the real atmospheric ^{14}C activity. Variations in the offset are about ±1 pMC (Figure 7b). This scenario exceeds the 1-σ limits of IntCal04 for large time intervals.
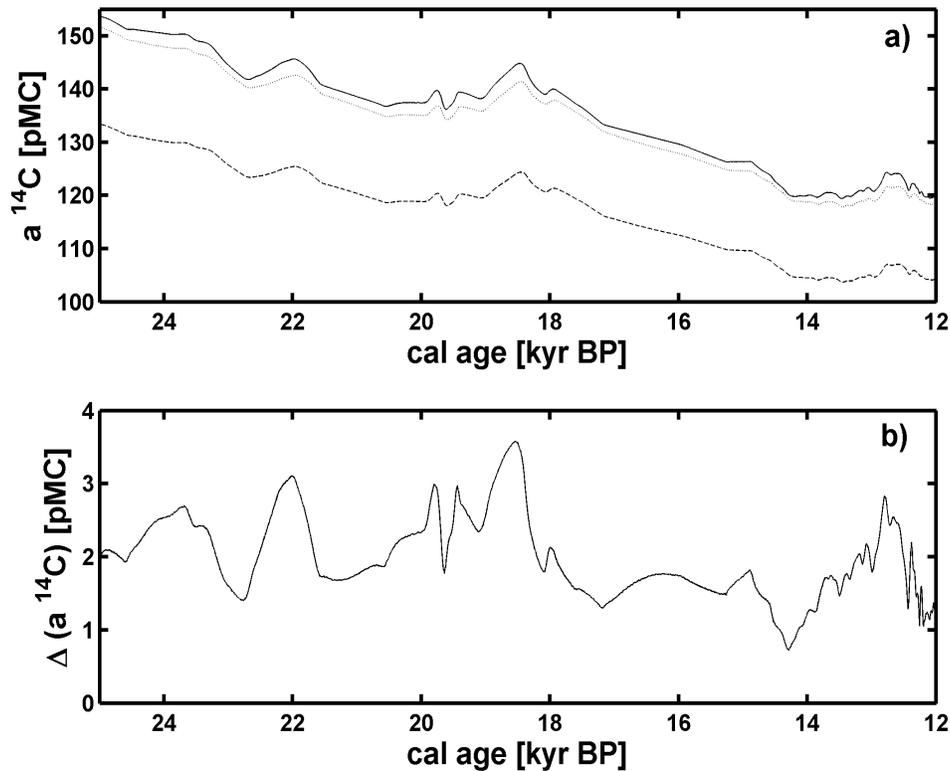
Figure 7 Assuming soil conditions, which is adapted for colder climate for the last 12 kyr, results in a mean total dcf of 12.06%. a) IntCal04 (straight line) and the artificially constructed ^{14}C data set (dashed line) are compared to the atmospheric ^{14}C activity reconstructed with the modeled ^{14}C data set (dotted line), which was computed with the mean dcf of the last 12 kyr. (b) The use of this dcf results in an underestimation of the atmospheric ^{14}C level in warmer climate conditions.

Both examples explored in this section are extreme cases with respect to the transition between the younger and the older SOM age spectrum. The offset between the ^{14}C activity of the atmosphere as derived from the stalagmite and the real atmospheric ^{14}C activity will be smaller for the time of the SOM modification, if a gradual change in the SOM age spectrum occurs. However, the offset is as large as described in the time the vegetation is constant. Furthermore, the chosen soil parameters are only exemplary, and hence, in reality the influence of the age spectrum of the vegetation can differ from that shown in this study.

CONCLUSION

In this study, we modeled the influence of the age spectrum of SOM above caves on the ^{14}C activity measured in stalagmites. We found that the integrating characteristic of the SOM, with respect to the carbon storage and the "memory" of past atmospheric radiogenic carbon composition, is responsible for the observed smoothed signal of the modeled stalagmite ^{14}C data set compared to the atmospheric ^{14}C signal. Furthermore, the age of the SOM influences the delay of atmospheric ^{14}C activity maximum and minimum values recorded in the stalagmite.

We showed also that variations in the dcf of up to ±1% can be found in stalagmites, even if all ^{14}C influencing sources and processes are constant over time. The magnitude of the dead carbon fraction

(dcf) results from 3 processes. First, the vegetation introduces a small amount of dead carbon, due to the carbon storage. In the case of a young reservoir, the dcf introduced by the vegetation is $dcf_{veg} = 0.22\%$ on average, while in the case of an older vegetation reservoir, it is $dcf_{veg} = 1.28\%$. The second process that influences the total dcf is carbon isotope fractionation between gaseous CO_2 and HCO^-_3 and between HCO^-_3 and $CaCO_3$. The third process is the dissolution of carbonate in the host-rock aquifer, during which the largest amount of dead carbon is introduced to the calcite of the stalagmite.

Furthermore, we investigated the deviations of the atmospheric ^{14}C activity between IntCal04 and the stalagmite-derived atmospheric ^{14}C activity for the period between 25 and 12 kyr BP. The cases with a constant age spectrum of SOM show a mean offset of 0.63 and 0.59 pMC for the younger and older SOM age spectrum, respectively. The deviations from the mean offsets depend on the timescale and strength of the variations of the atmospheric ^{14}C activity. However, the 1-σ limits of IntCal04 will only be exceeded if the constant SOM age spectrum is significantly older than the values we used. The deviation between the atmospheric ^{14}C level as derived with a stalagmite and IntCal04 originate from the simplified treatment of translating the stalagmite signal into an atmospheric one (Equation 6). The use of the dcf neglects the smoothing character of the age spectrum of vegetation and SOM, which are well described by Equations 1 to 5.

For reconstructing the past atmospheric ^{14}C activity, it is suggested to use stalagmites from caves, which very likely did not experience vegetation changes during the past or where vegetation changes are supposed to be small. An estimate of vegetation changes in the area of the cave can be given by studies of nearby pollen. Furthermore, it is better to use stalagmites in caves with a relative young age spectrum of SOM, because then the derived atmospheric ^{14}C activity does not suffer under large variations as for older SOM reservoirs above the cave. The problem with a young SOM reservoir is that it frequently means that vegetation cover is relative small. In caves with such soil, the growth rate of stalagmites is often not high, which complicates such a ^{14}C study due to temporal resolution limits; thus, one has to accept compromises in that relationship.

Additional attention should be paid to the fact that in this model approach the observed deviations between IntCal04 and the atmospheric ^{14}C activity as derived from the artificial stalagmite ^{14}C data set originate from the SOM age spectrum alone, even when the SOM age spectrum is constant. In our study, we focussed only on the age spectrum of the vegetation/SOM and neglected changes in the open versus closed carbonate dissolution process as well as changes in soil-air pCO_2. Both processes have the potential to influence the host-rock contribution significantly and, hence, to introduce large deviations between the real atmospheric ^{14}C composition and the ^{14}C level of the atmosphere as derived with a stalagmite, if a constant total dcf is assumed. No evaluation of the impact on the stalagmite ^{14}C record of these both processes was done. However, it seems that changes in the host-rock contribution are more important on the total dcf than changes in the age spectrum of SOM, because the host rock is the dominant source of the dead carbon. In addition, neither absolute age nor ^{14}C activity measurement uncertainties are included in this study.

ACKNOWLEDGMENTS

REFERENCES

Beck JW, Richards DA, Edwards RL, Silverman BW, Smart PL, Donahue DJ, Hererra-Osterheld S, Burr G.S, Calsoyas L, Jull AJT, Biddulph D. 2001. Extremely large variations of atmospheric ^{14}C concentration during the last glacial period. *Science* 292(5526): 2453–8.

Borsato A. 1997. Dripwater monitoring at Grotta di Ernesto (NE Italy): a contribution to the understanding of karst hydrology and the kinetics of carbonate dissolution. In: *Proceedings of the 12th International Congress of Speleology.* Volume 2. p 57–60.

Borsato A, Frisia S, Fairchild IJ, Somogyi A, Susini J. 2007. Trace element distribution in annual stalagmite laminae mapped by micrometer-resolution X-ray fluorescence: implications for incorporation of environmentally significant species. *Geochimica et Cosmochimica Acta* 71(6):1494–512.

Broecker WS, Olson EA, Orr PC. 1960. Radiocarbon measurements and annual rings in cave formations. *Nature* 185(4706):93–4.

Dörr H, Münnich KO. 1986. Annual variations of the ^{14}C content. *Radiocarbon* 28(2A):338–45.

Dreybrodt W. 1988. *Processes in Karst Systems - Physics, Chemistry and Geology.* Berlin: Springer Verlag. 288 p.

Dulinski M, Rozanski K. 1990. Formation of ^{13}C/^{12}C isotope ratios in speleothems: a semi-dynamic model. *Radiocarbon* 32(1):7–16.

Edwards RL, Chen JH, Wasserburg GJ. 1987. [238]U–[234]U–[230]Th–[232]Th systematics and the precise measurement of time over the past 500,000 years. *Earth and Planetary Science Letters* 81(2–3)175–92.

Fairchild IJ, Borsato A, Tooth AF, Frisia S, Hawkesworth CJ, Huang Y, McDermott F, Spiro B. 2000. Controls on trace element (Sr-Mg) compositions of carbonate cave water: implications for speleothem climatic records. *Chemical Geology* 166(3–4):255–69.

Fohlmeister J, Schröder-Ritzrau A, Spötl C, Frisia S, Miorandi R, Kromer B, Mangini A. 2010. The influences of hydrology on the radiogenic and stable carbon isotope composition of cave drip water, Grotta di Ernesto (Italy). *Radiocarbon* 52(4)1529–44.

Franke HW, Münnich KO, Vogel JC. 1959. Erste Ergebnisse von Kohlenstoffisotopenmessungen an Kalksinter. *Die Höhle* 10:17–22.

Franke WF. 1951. Altersbestimmung von Kalzitkonkretionen mit radioaktivem Kohlenstoff. *Naturwissenschaften* 38:527–8.

Frisia S, Borsato A, Preto N, McDermott F. 2003. Late Holocene annual growth in three alpine stalagmite records the influence of solar activity and the North Atlantic Oscillation on winter climate. *Earth and Planetary Science Letters* 216(3):411–24.

Frisia S, Borsato A, Fairchild IJ, Susini S. 2005. Variations in atmospheric sulphate recorded in stalagmites by synchrotron micro-XRF and XANES analyses. *Earth and Planetary Science Letters* 235(3–4):729–40.

Frisia S, Fairchild IJ, Fohlmeister J, Miorandi R, Spötl C, Borsato A. 2011. Carbon mass-balance modelling and carbon isotope exchange processes in dynamic caves. *Geochimica et Cosmochimica Acta* 75(2):380–400.

Garrels RM, Christ CL. 1965. *Solutions, Minerals and Equilibria.* New York: Harper & Row. 450 p.

Genty D, Massault M. 1997. Bomb ^{14}C recorded in laminated speleothems: calculations of dead carbon proportion. *Radiocarbon* 39(1):33–48.

Genty D, Massault M. 1999. Carbon transfer dynamics from bomb-^{14}C and δ^{13}C time series of a laminated stalagmite from SW France—modelling and comparison with other stalagmite records. *Geochimica et Cosmochimica Acta* 63(10):1537–48.

Genty D, Vokal B, Obelic B, Massault M. 1998. Bomb ^{14}C time history recorded in two modern stalagmites—importance for soil organic matter dynamics and bomb ^{14}C distribution over continents. *Earth and Planetary Science Letters* 160(3–4):795–809.

Genty D, Massault M, Gilmour M, Baker A, Verheyden S, Kepens E. 1999. Calculation of past dead carbon proportion and variability by the comparison of AMS ^{14}C and TIMS U/Th ages on two Holocene stalagmites. *Radiocarbon* 41(3):251–70.

Genty D, Baker A, Massault M, Proctor C, Gilmour M, Pons-Branchu E, Hamelin B. 2001. Dead carbon in stalagmite: carbonate bedrock paleodissolution vs. ageing of soil organic matter. Implications for ^{13}C variations in speleothems. *Geochimica et Cosmochimica Acta* 65(20):3443–57.

Geyh MA, Franke HW. 1970. Zur Wachstumsgeschwindigkeit von Stalagmiten. *Atompraxis* 16:46–8.

Geyh MA, Schlüchter C. 1998. Calibration of the ^{14}C time scale beyond 22,000 BP. *Radiocarbon* 40(1): 475–82.

Goslar T, Hercman H, Pazdur A. 2000. Comparison of U-series and radiocarbon dates of speleothems. *Radiocarbon* 42(3):403–14.

Harrison K, Broecker W, Bonani G. 1993. A strategy for estimating the impact of CO_2 fertilization on soil carbon storage. *Global Biogeochemical Cycles* 7(1):69–80.

Hendy CH. 1970. The use of ^{14}C in the study of cave processes. In: Olsson IU, editor. *Radiocarbon Variations and Absolute Chronology.* New York: Wiley Interscience Division. p 419–43.

Hendy CH. 1971. The isotopic geochemistry of speleothems—I. The calculation of the effects of different modes of formation on the isotopic composition of speleothems and their applicability as palaeoclimatic indicators. *Geochimica et Cosmochimica Acta* 35(8): 801–24.

Hendy CH, Wilson AT. 1968. Palaeoclimatic data from speleothems. *Nature* 219(5149):48–51.

Hoffmann DL, Beck JW, Richards D, Smart PL, Singarayer JS, Ketchmark T, Hawkesworth CJ. 2010. Towards radiocarbon calibration beyond 28 ka using speleothems from the Bahamas. *Earth and Planetary Science Letters* 289(1–2):1–10.

Huang YM, Fairchild IJ, Borsato A, Frisia S, Cassidy NJ, McDermott F, Hawkesworth CJ. 2001. Seasonal variations in Sr, Mg and P in modern speleothems (Grotta di Ernesto, Italy). *Chemical Geology* 175(3–4):429–48.

Levin I, Kromer B. 2004. The tropospheric ^{14}CO$_2$ level in mid-latitudes of the Northern Hemisphere (1959–2003. *Radiocarbon* 46(3):1261–72.

Levin I, Naegler T, Kromer B, Diehl M, Francey RJ, Gomez-Pelaez AJ, Steele LP, Wagenbach D, Weller R, Worthy DS. 2010. Observations and modelling of the global distribution and long-term trend of atmospheric ^{14}CO$_2$. *Tellus B* 62(1):26–46.

Li W-X, Lundberg J, Dickin AP, Ford DC, Schwarcz HP, McNutt R, Williams D. 1989. High-precision mass-spectrometric uranium-series dating of cave deposits and implications for palaeoclimate studies. *Nature* 339(6225):534–6.

Libby WF, Anderson EC, Arnold JR. 1949. Age determination by radiocarbon content: world-wide assay of natural radiocarbon. *Science* 109(2827):227–28.

Mattey D, Lowry D, Duffet J, Fisher R, Hodge E, Frisia S. 2008. A 53 year seasonally resolved oxygen and carbon isotope record from a modern Gibraltar speleothem: reconstructed drip water and relationship to local precipitation. *Earth and Planetary Science Letters* 269(1–2):80–95.

McDermott F. 2004. Palaeo-climate reconstruction from stable isotope variations in speleothems: a review. *Quaternary Science Reviews* 23(7–8):901–18.

McDermott F, Frisia S, Huang Y, Longinelli A, Spiro B, Heaton THE, Hawkesworth CJ, Borsato A, Keppens E, Fairchild IJ, van der Borg K, Verheyden S, Selmo EM. 1999. Holocene climate variability in Europe: evidence from δ^{18}O, textural and extension-rate variations in three speleothems. *Quaternary Science Reviews* 18(8–9):1021–38.

Mook WG, de Vries JJ. 2000. *Environmental Isotopes in the Hydrological Cycle Principles and Applications - Volume I: Introduction - Theory, Methods, Review.* Vienna: IAEA.

Reimer PJ, Baillie MGL, Bard E, Bayliss A, Beck JW, Bertrand CJH, Blackwell PG, Buck CE, Burr GS, Cutler KB, Damon PE, Edwards RL, Fairbanks RG, Friedrich M, Guilderson TP, Hogg AG, Hughen KA, Kromer B, McCormac G, Manning S, Bronk Ramsey C, Reimer RW, Remmele S, Southon JR, Stuiver M, Talamo S, Taylor FW, van der Plicht J, Weyhenmeyer CE. 2004. IntCal04 terrestrial radiocarbon age cali-

bration, 0–26 cal kyr BP. *Radiocarbon* 46(3):1029–58.

Saliège JF, Fontes JC. 1984. Essai de détermination expérimentale du fractionnement des isotopes ^{13}C et ^{14}C du carbone au cours de processus naturels. *International Journal of Applied Radiation and Isotopes* 35(1):55–62.

Salomons W, Mook WG. 1986. Isotope geochemistry of carbonates in the weathering zone. In: Fritz P, Fontes JC, editors. *Handbook of Isotope Geochemistry, 1 The Terrestrial Environment.* Amsterdam: Elsevier. p 239–70.

Scholz D, Hoffmann D. 2008. ^{230}Th/U-dating of fossil reef corals and speleothems. *Quaternary Science Journal* 57(1–2):52–77.

Schwarcz HP. 1986. Geochronology and isotopic geochemistry of speleothems. In: Fritz P, Fontes JC, editors. *Handbook of Isotope Geochemistry, 1 The Terrestrial Environment.* Amsterdam: Elsevier. p 271–303.

Skog G. 2007. The single stage AMS machine at Lund University: status report. *Nuclear Instruments and Methods in Physics Research B* 259(1):1–6.

Smith CL, Fairchild IJ, Spötl C, Frisia S, Borsato A, Moreton SG, Wynn PM. 2009. Chronology building using objective identification of annual signals in trace element profiles of stalagmites. *Quaternary Geochronology* 4(1):11–21.

Tegen I, Dörr H. 1996. ^{14}C measurements of soil organic matter, soil CO$_2$ and dissolved organic carbon. *Radiocarbon* 38(2):247–51.

Thornthwaite CW. 1948. An approach toward a rational classification of climate. *Geographical Review* 38(1):55–94.

Trumbore SE. 2000. Age of soil organic matter and soil respiration: radiocarbon constraints on belowground C dynamics. *Ecological Applications* 10(2):399–411.

Trumbore SE, Davidson EA, de Camargo PB, Nepstad DC, Martinelli LA. 1995. Belowground cycling of carbon in forests and pastures of eastern Amazonia. *Global Biogeochemical Cycles* 9(4):515–28.

Vogel JC, Kronfeld J. 1997. Calibration of radiocarbon dates for the Late Pleistocene using U/Th dates on stalagmites. *Radiocarbon* 39(1):27–32.

Wackerbarth A, Scholz D, Fohlmeister J, Mangini A. 2010. Modelling the δ^{18}O value of cave drip water and speleothem calcite. *Earth and Planetary Science Letters* 299(3–4):367– 97.

Wendt I, Stahl W, Geyh MA, Fauth F. 1967. Model experiments for ^{14}C water-age determinations. In: *Isotopes in Hydrology, Proceedings of the IAEA.* STI/PUB/141. Vienna: IAEA. p 321–37.

Wigley TML. 1975. Carbon-14 dating of groundwater from closed and open systems. *Water Resources Research* 11(2):324–8.